Supplementary Information

Enhanced Visible-Light Degradation over N-CDs-Modified Bi_7VO_{13}: Role of Interfacial Charge Transport

Pengyuan Liu,[a] Ziyu Song,[a] Bicheng Ji,[a] Junfu Xiong,[b] Xicheng Li,[a] Changzheng Wang*[a]
[a] Institute of Advanced Materials, Beijing Key Laboratory of Functional Materials for Building Structure and Environment Remediation, School of Environment and Energy Engineering, Beijing University of Civil Engineering and Architecture, Beijing, 100044, China. E-mail: changzhwang@163.com
[b] Luzhou Xinglu Environmental Protection Development Co., Ltd, Luzhou, 646000, China

*Corresponding author: Changzheng Wang(changzhwang@163.com)

Table of Contents

Supplementary Text **3**
Text S1 Experimental reagents 3
Text S2 Experimental equipment 3
Text S3 Density functional theory (DFT) calculation 3
Supplementary Equation **4**
Equation S1 Degradation efficiency calculation formula 4
Equation S2 The pseudo-first-order kinetic rate constant calculation formula 4
Equation S3 Tauc equation 4
Equation S4 Internal electric field (IEF) intensity 4
Equation S5 Charge separation efficiency 4
Equation S6 Definition of the Fukui function 4
Equation S7 Fukui function nucleophilic attack 4
Equation S8 Fukui function electrophilic attack 4
Equation S9 Fukui function radical attack 4
Equation S10 Formula for calculating local softness 4
Equation S11 Local softness nucleophilic attack 4
Equation S12 Local softness electrophilic attack 5
Equation S13 Local softness radical attack 5
Equation S14 Definition of the hyper-softness 5
Supplementary Figure **6**
Figure S1 SEM image of N-CB(4) 6
Figure S2 TEM image of Bi_7VO_{13} 6
Figure S3 XPS spectrum of Bi_7VO_{13} and N-CB(4) 6
Figure S4 C 1s peak spectrum of Bi_7VO_{13} 7
Figure S5 I-T curves for Bi_7VO_{13} and N-CB(4) 7
Figure S6 EIS low-frequency region images of Bi_7VO_{13} and N-CB(4) (a-b) 7
Figure S7 Photocatalytic degradation of tetracycline hydrochloride by Bi_7VO_{13} and N-CB(X) (a) Photocatalytic degradation curve (b) Pseudoneventh-order rate constant plot 8
Figure S8 Adsorption curves of Bi_7VO_{13} and N-CB(4) for TCH under dark conditions 8
Supplementary Table **9**
Table S1 Condensed local softness and hyper-softness calculation results of TCH 9
Table S2 Condensed fukui function calculation results. 11
The mass spectrometry data of TCH and the intermediate products **13**
Supplementary references **18**

Supplementary Text

Text S1 Experimental reagents

The medicines used include Tetracycline hydrochloride ($C_{22}H_{25}ClN_2O_8$，99%) were purchased from Macklin Biochemical Co..And Anhydrous ethanol (C_2H_6O, 99%), Sodium hydroxide (NaOH, 99%), Hydrochloric acid (HCl, 99%), Sodium carbonate ($NaSO_4$, 99%), D-mannitol ($C_6H_{14}O_6$, 99%), Ammonium metavanadate (NH_4VO_3, 99%), Urea (CH_4N_2O, 99%), Bismuth nitrate pentahydrate ($Bi(NO_3)_3·5H_2O$, 99%), Citric acid ($C_6H_8O_7$, 99%) were of analytical grade and used as received without further purification.

Text S2 Experimental equipment

X-ray diffraction (XRD) patterns of different samples were recorded using the XRD-6100 (XRD; Shimadzu, Japan). The morphology and surface composition were observed using a scanning electron microscope (ZEISS GeminiSEM 360). The morphology and composition of this sample were explored using transmission electron microscopy (TEM, TEOL H7650, Japan). EDS data was obtained from TEM analysis for elemental content analysis. The chemical states of the samples were measured by using X-ray photoelectron spectroscopy (XPS, Thermo ESCALAB250Xi, USA), and the binding energy of the C 1s peak at 284.8 eV was taken as an internal standard. The absorbance properties of the photoanode materials were tested using UV-visible diffuse reflectance spectroscopy (DRS, Shimadzu UV-2600, Japan) with a measurement wavelength range of 200-800 nm. The cyclic voltammetry , electrochemical impedance spectroscopy, linear sweep voltammetry, transient photocurrent, open circuit voltage decay and Mott-schottky tests were carried out by an electrochemical workstation (CHI660E electrochemical station, Shanghai Chenhua, China) using a threeelectrode system. Functional group transformations and chemical bond modifications in the photocatalytic materials were characterized by fourier transform infrared spectroscopy (FT-IR, Nicolet iS5, Thermo Fisher Scientific, USA). LC-MS (Thermo Fisher-UltiMate 3000 HPLC) utilises liquid chromatography as the separation system and mass spectrometry as the detection system to detect the intermediates produced during the degradation of TCH.

Text S3 Density functional theory (DFT) calculation

Geometry optimization and single-point energy were executed at the B3LYP/6-31 + G(d,p) level of theory using the Gaussian 16W software. The regioselectivity of ROS attacks on TCH molecules is explained based on the Fukui index and local softness. Specifically, the Fukui function plays an important role in DFT calculation and is widely used to predict reaction sites for electrophilic, nucleophilic, and radical attacks.

To address the limitation that the Fukui function can only compare the susceptibility of sites within the same molecule and cannot evaluate the reactivity differences between sites across different molecules, local softness was introduced as a novel metric to assess the reactivity variations of deprotonated TCH molecules toward reactive oxygen species.

Supplementary Equation

Equation S1 Degradation efficiency calculation formula

$$\text{Degradation}(\%) = (C_0 - C_t)/C_0 \times 100\% \#(S1)$$

Herein, C_0 denotes the initial concentration of the solution, while C_t represents the concentration at time t.

Equation S2 The pseudo-first-order kinetic rate constant calculation formula

$$-\ln(C_t - C_0) = kt \#(S2)$$

Herein, C_0 denotes the initial concentration of the solution, while C_t represents the concentration at time t.

Equation S3 Tauc equation

$$\alpha h\nu = A(h\nu - Eg)^{1/n} \#(S3)$$

Here, α, h, ν, A and n denote the absorption coefficient, Planck's constant, incident photon energy, proportionality constant and dimensionless constant respectively. For the material employed in this experiment, n = 2.

Equation S4 Internal electric field (IEF) intensity

$$E = (-2V_S\rho/\varepsilon\varepsilon_0)^{1/2} \#(S4)$$

Herein, E, V_S, ρ, ε and ε_0 represent the IEF magnitude, surface potential, surface charge density, low-frequency dielectric constant, and vacuum permittivity, respectively.

Equation S5 Charge separation efficiency

$$\eta = J_{SO_4^{2-}}/J_{SO_3^{2-}} \#(S5)$$

where $J_{SO_4^{2-}}$ and $J_{SO_3^{2-}}$ are the photocurrent densities measured under different electrolyte conditions.

Equation S6 Definition of the Fukui function

$$f(r) = \left[\frac{\partial\rho(r)}{\partial N}\right]_v \#(S6)$$

Where $\rho(r)$ was the electron density at a point r in space, N was electron number in present system, the constant term ν in the partial derivative was external potential.[1] In the condensed version of Fukui function, atomic population number was used to represent the amount of electron density distribution around an atom.

Equation S7 Fukui function nucleophilic attack

$$f_k^+ = q_N^k - q_{N+1}^k \#(S7)$$

Equation S8 Fukui function electrophilic attack

$$f_k^- = q_{N-1}^k - q_N^k \#(S8)$$

Equation S9 Fukui function radical attack

$$f_k^0 = (q_{N-1}^k - q_{N+1}^k)/2 \#(S9)$$

Where q^k was the atom charge of atom K at corresponding state, and the values of Fukui index of the reactive sites were usually larger than other regions.

To address the limitation that the Fukui function can only compare the susceptibility of sites within the same molecule and cannot evaluate the reactivity differences between sites across different molecules, local softness was introduced as a novel metric to assess the reactivity variations of deprotonated TCH molecules toward reactive oxygen species (ROS).[2]

Equation S10 Formula for calculating local softness

$$LS = S * f(r) \#(S10)$$

Where S was Softness of the molecule. Similar to the Fukui function

Equation S11 Local softness nucleophilic attack

$$s_k^+ = S * (q_N^k - q_{N+1}^k) \#(S11)$$

Equation S12 Local softness electrophilic attack

$$s_k^- = S * (q_{N-1}^k - q_N^k) \#(S12)$$

Equation S13 Local softness radical attack

$$s_k^0 = S * (q_{N-1}^k - q_{N+1}^k)/2 \#(S13)$$

Hyper-softness, an improvement on the dual descriptor, can also describe the electrophilic and nucleophilic reactivity of molecular sites. We incorporated this parameter as a parallel metric to evaluate the inter-molecular reactivity of deprotonated TCH species, providing a more comprehensive assessment.

Equation S14 Definition of the hyper-softness

$$s_k^2 = S^2 * DD_k \#(S14)$$

Where DDk was the dual descriptor of atom K at corresponding state.

In this study, the isosurfaces and isopotential maps of the Fukui function, softness and hyper-softness on the surface of the TCH molecule were visualized by using Multiwfn in combination with VMD.[3]

Supplementary Figure

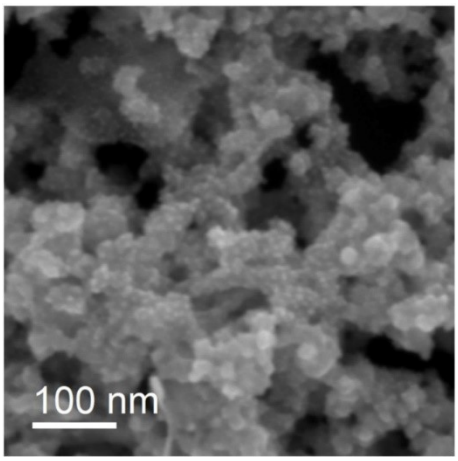

Figure S1 SEM image of N-CB(4)

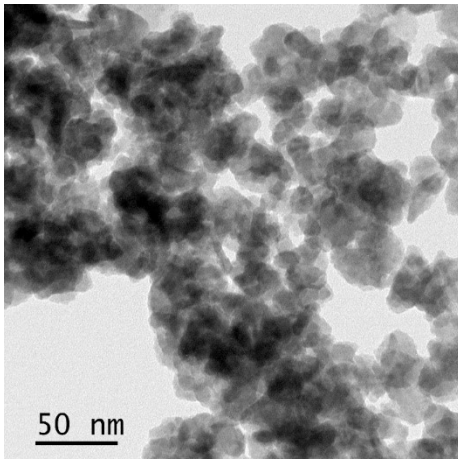

Figure S2 TEM image of Bi_7VO_{13}

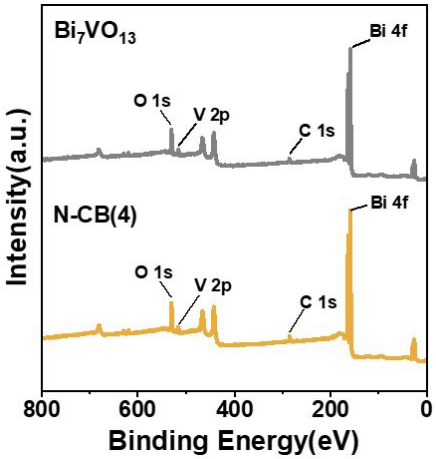

Figure S3 XPS spectrum of Bi_7VO_{13} and N-CB(4)

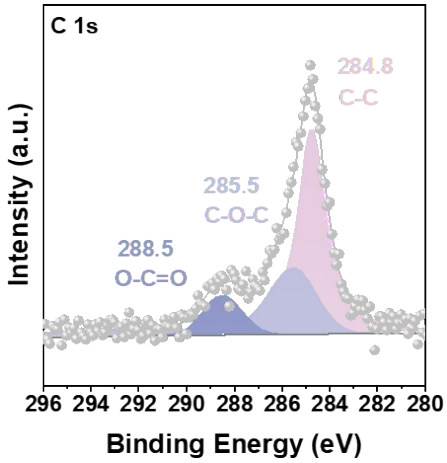

Figure S4 C 1s peak spectrum of Bi_7VO_{13}

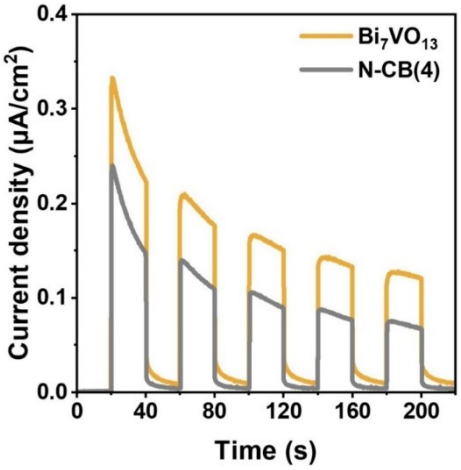

Figure S5 I-T curves for Bi_7VO_{13} and N-CB(4)

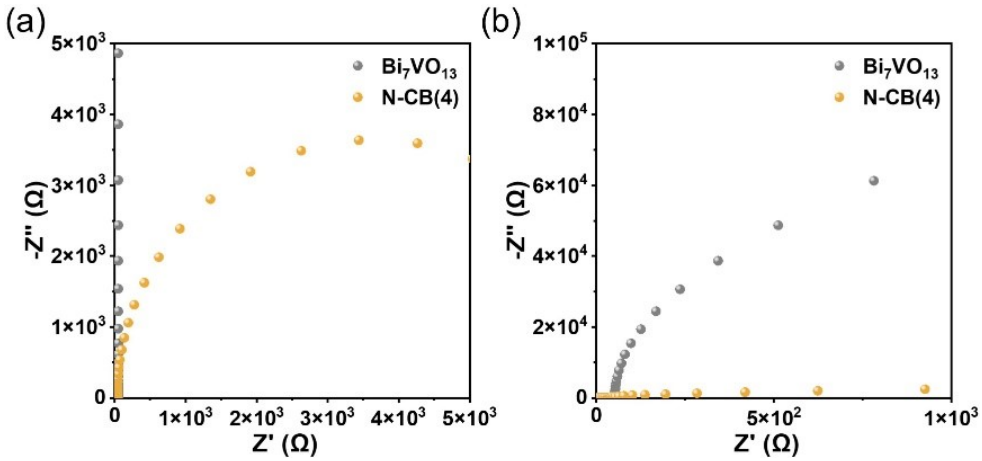

Figure S6 EIS low-frequency region images of Bi_7VO_{13} and N-CB(4) (a-b)

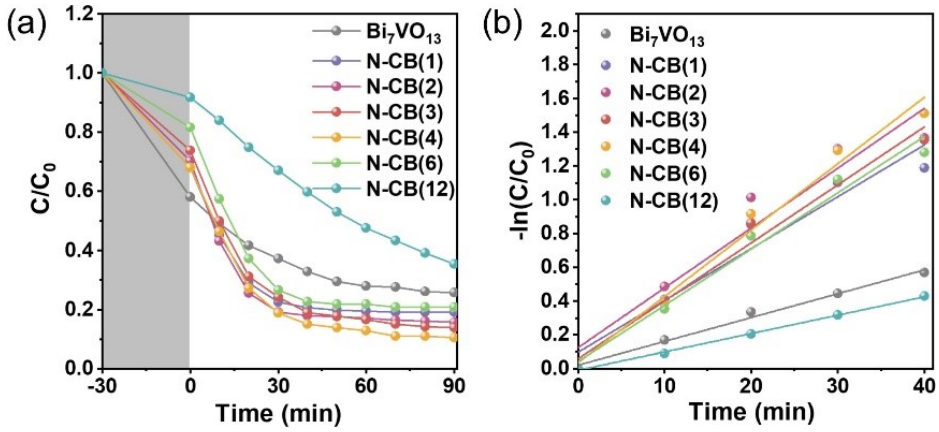

Figure S7 Photocatalytic degradation of tetracycline hydrochloride by Bi_7VO_{13} and N-CB(X) (a) Photocatalytic degradation curve (b) Pseudoneventh-order rate constant plot

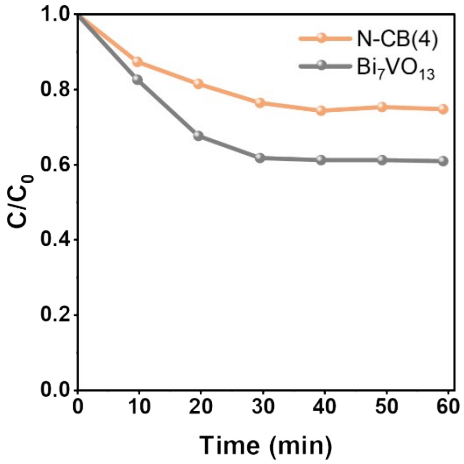

Figure S8 Adsorption curves of Bi_7VO_{13} and N-CB(4) for TCH under dark conditions

Supplementary Table

Table S1 Condensed local softness and hyper-softness calculation results of TCH

NO.(Atom)	s^-	s^+	s^0	s^2
1(C)	0.0262	0.0536	0.0399	0.2291
2(C)	0.0251	0.266	0.1456	2.0161
3(C)	0.0133	0.7076	0.3605	5.8089
4(C)	0.0057	0.217	0.1113	1.7673
5(C)	0.0046	0.2848	0.1447	2.3444
6(C)	0.01	0.2076	0.1088	1.6537
7(H)	0.0056	0.111	0.0583	0.8819
8(C)	0.0121	0.4794	0.2457	3.9101
9(C)	0.0102	0.2363	0.1232	1.8916
10(C)	0.0103	0.3355	0.1729	2.721
11(H)	0.1022	0.0609	0.0816	-0.3458
12(H)	0.0061	0.2041	0.1051	1.6565
13(H)	0.0056	0.1263	0.066	1.0095
14(C)	0.03	0.122	0.076	0.7697
15(C)	0.1317	0.0274	0.0795	-0.873
16(C)	0.0505	0.0414	0.046	-0.0767
17(C)	0.2334	0.0277	0.1305	-1.7212
18(C)	0.0682	0.083	0.0756	0.124
19(C)	0.2467	0.0458	0.1463	-1.6806
20(C)	0.0224	0.9848	0.5036	8.0529
21(O)	0.0382	1.012	0.5251	8.1475
22(C)	0.0935	0.1362	0.1149	0.3569
23(O)	0.2423	0.2153	0.2288	-0.2257
24(C)	0.0503	0.0205	0.0354	-0.2495
25(O)	0.0963	0.0359	0.0661	-0.5051
26(N)	0.0454	0.0182	0.0318	-0.2276
27(H)	0.0394	0.014	0.0267	-0.2126
28(H)	0.0314	0.0108	0.0211	-0.1726
29(O)	0.1492	0.0697	0.1095	-0.6653
30(H)	0.098	0.0298	0.0639	-0.5713
31(N)	2.1428	0.0149	1.0789	-17.8043
32(C)	0.4821	0.0121	0.2471	-3.9325

NO.(Atom)	s^-	s^+	s^0	s^2
33(H)	0.6558	0.0124	0.3341	-5.3828
34(H)	0.3486	0.0116	0.1801	-2.82
35(H)	0.3202	0.0104	0.1653	-2.5924
36(C)	0.4662	0.0148	0.2405	-3.7761
37(H)	0.3809	0.0138	0.1973	-3.0716
38(H)	0.6414	0.0154	0.3284	-5.2379
39(H)	0.273	0.0227	0.1478	-2.0939
40(C)	0.0105	0.0416	0.0261	0.2604
41(O)	0.0099	0.0885	0.0492	0.6576
42(H)	0.01	0.066	0.038	0.4679
43(C)	0.0069	0.0414	0.0242	0.289
44(H)	0.0072	0.0405	0.0238	0.2783
45(H)	0.0071	0.0444	0.0257	0.3118
46(H)	0.0101	0.0436	0.0269	0.2807
47(O)	0.0337	0.5483	0.291	4.306
48(H)	0.0178	0.2286	0.1232	1.7642
49(O)	0.0574	0.189	0.1232	1.1006
50(H)	0.0623	0.1107	0.0865	0.4053
51(H)	0.0632	0.0627	0.063	-0.0042
52(H)	0.0341	0.103	0.0685	0.5762
53(H)	0.1536	0.0658	0.1097	-0.7347
54(H)	0.2541	0.0403	0.1472	-1.7891
55(O)	0.0089	0.2292	0.119	1.8433
56(H)	0.0046	0.1087	0.0566	0.8714

Table S2 Condensed fukui function calculation results.

NO.(Atom)	q(N)	q(N+1)	q(N-1)	f^-	f^+	f^0
1(C)	-0.0155	-0.0219	-0.0124	0.0031	0.0064	0.0048
2(C)	-0.0534	-0.0852	-0.0504	0.003	0.0318	0.0174
3(C)	0.1052	0.0206	0.1068	0.0016	0.0846	0.0431
4(C)	-0.039	-0.0649	-0.0383	0.0007	0.0259	0.0133
5(C)	0.0061	-0.028	0.0066	0.0006	0.034	0.0173
6(C)	-0.0523	-0.0771	-0.0511	0.0012	0.0248	0.013
7(H)	0.0528	0.0395	0.0535	0.0007	0.0133	0.007
8(C)	-0.0221	-0.0794	-0.0206	0.0014	0.0573	0.0294
9(C)	-0.0551	-0.0833	-0.0539	0.0012	0.0282	0.0147
10(C)	0.088	0.0479	0.0893	0.0012	0.0401	0.0207
11(H)	0.0146	0.0074	0.0269	0.0122	0.0073	0.0097
12(H)	0.0618	0.0374	0.0626	0.0007	0.0244	0.0126
13(H)	0.0656	0.0505	0.0663	0.0007	0.0151	0.0079
14(C)	0.0776	0.0631	0.0812	0.0036	0.0146	0.0091
15(C)	-0.0162	-0.0195	-0.0004	0.0157	0.0033	0.0095
16(C)	-0.0517	-0.0566	-0.0456	0.006	0.0049	0.0055
17(C)	0.0365	0.0332	0.0644	0.0279	0.0033	0.0156
18(C)	0.1311	0.1212	0.1392	0.0081	0.0099	0.009
19(C)	-0.0647	-0.0702	-0.0352	0.0295	0.0055	0.0175
20(C)	0.1256	0.0079	0.1283	0.0027	0.1177	0.0602
21(O)	-0.2892	-0.4102	-0.2847	0.0046	0.1209	0.0628
22(C)	0.1363	0.12	0.1475	0.0112	0.0163	0.0137
23(O)	-0.3455	-0.3713	-0.3166	0.029	0.0257	0.0273
24(C)	0.1518	0.1494	0.1578	0.006	0.0024	0.0042
25(O)	-0.4242	-0.4285	-0.4127	0.0115	0.0043	0.0079
26(N)	-0.1051	-0.1073	-0.0997	0.0054	0.0022	0.0038
27(H)	0.1558	0.1541	0.1605	0.0047	0.0017	0.0032
28(H)	0.1581	0.1568	0.1618	0.0038	0.0013	0.0025
29(O)	-0.1545	-0.1629	-0.1367	0.0178	0.0083	0.0131
30(H)	0.2097	0.2061	0.2214	0.0117	0.0036	0.0076
31(N)	-0.0959	-0.0976	0.1602	0.2561	0.0018	0.1289
32(C)	-0.037	-0.0384	0.0206	0.0576	0.0014	0.0295
33(H)	0.0304	0.0289	0.1088	0.0784	0.0015	0.0399

NO.(Atom)	q(N)	q(N+1)	q(N-1)	f^-	f^+	f^0
34(H)	0.04	0.0386	0.0816	0.0417	0.0014	0.0215
35(H)	0.0419	0.0407	0.0802	0.0383	0.0012	0.0198
36(C)	-0.0553	-0.057	0.0004	0.0557	0.0018	0.0287
37(H)	0.0371	0.0355	0.0827	0.0455	0.0016	0.0236
38(H)	0.0176	0.0157	0.0942	0.0767	0.0018	0.0393
39(H)	0.0197	0.017	0.0524	0.0326	0.0027	0.0177
40(C)	0.0946	0.0896	0.0958	0.0013	0.005	0.0031
41(O)	-0.2549	-0.2654	-0.2537	0.0012	0.0106	0.0059
42(H)	0.1689	0.161	0.1701	0.0012	0.0079	0.0045
43(C)	-0.0861	-0.0911	-0.0853	0.0008	0.005	0.0029
44(H)	0.0433	0.0384	0.0441	0.0009	0.0048	0.0028
45(H)	0.0389	0.0336	0.0398	0.0008	0.0053	0.0031
46(H)	0.0438	0.0386	0.045	0.0012	0.0052	0.0032
47(O)	-0.2024	-0.2679	-0.1984	0.004	0.0655	0.0348
48(H)	0.1104	0.083	0.1125	0.0021	0.0273	0.0147
49(O)	-0.2105	-0.2331	-0.2037	0.0069	0.0226	0.0147
50(H)	0.1718	0.1586	0.1792	0.0074	0.0132	0.0103
51(H)	0.0447	0.0372	0.0522	0.0076	0.0075	0.0075
52(H)	0.0433	0.031	0.0474	0.0041	0.0123	0.0082
53(H)	0.0485	0.0406	0.0669	0.0184	0.0079	0.0131
54(H)	0.0646	0.0598	0.095	0.0304	0.0048	0.0176
55(O)	-0.2045	-0.2319	-0.2035	0.0011	0.0274	0.0142
56(H)	0.1996	0.1866	0.2002	0.0005	0.013	0.0068

The mass spectrometry data of TCH and the intermediate products

m/z =445

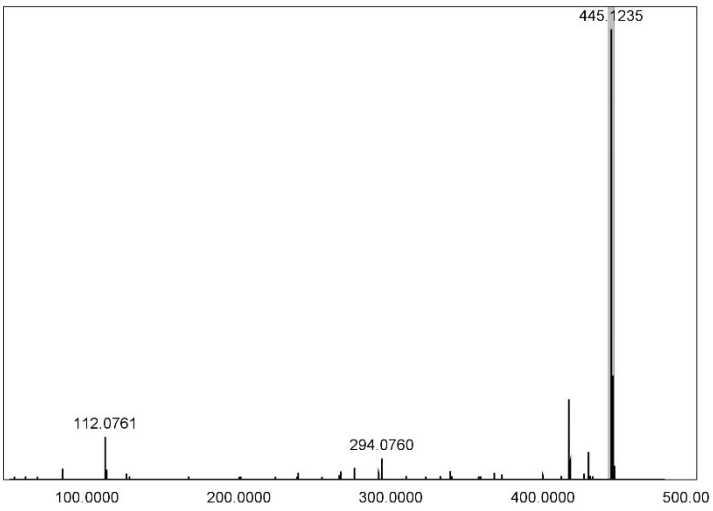

m/z =427

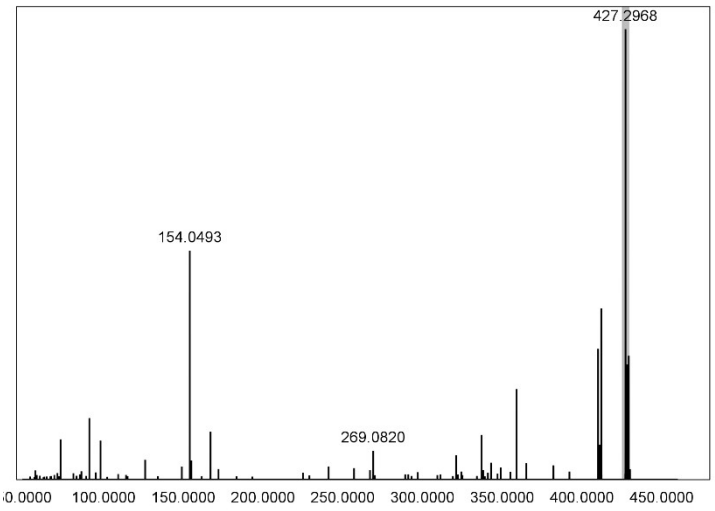

m/z =340

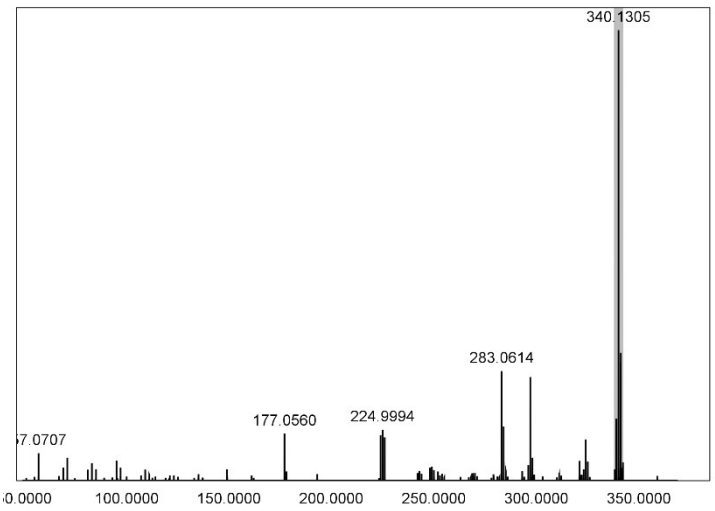

m/z =327

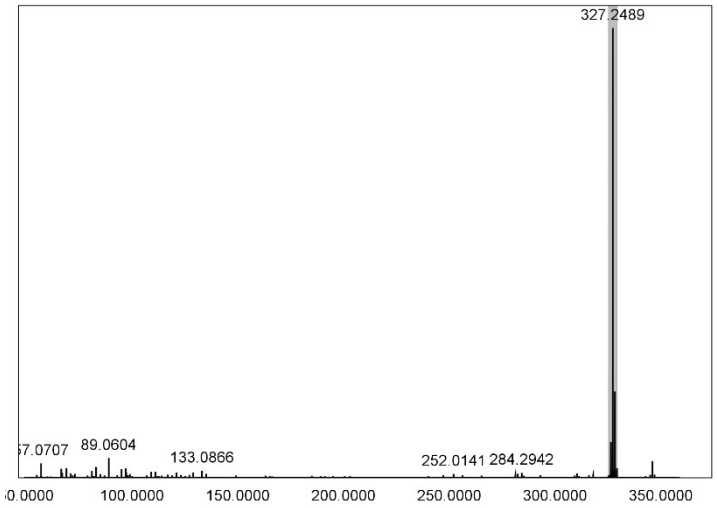

m/z =190

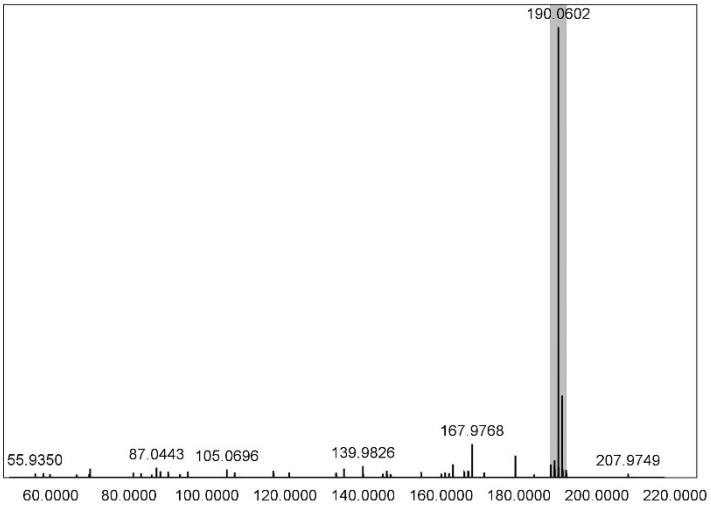

m/z =165

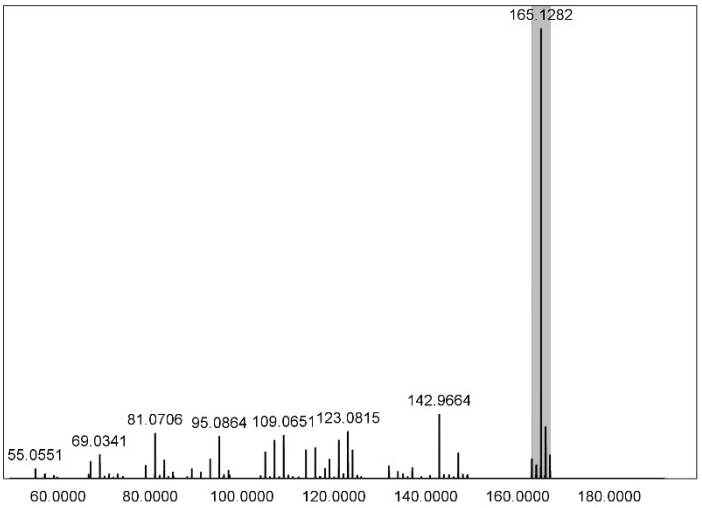

m/z =114

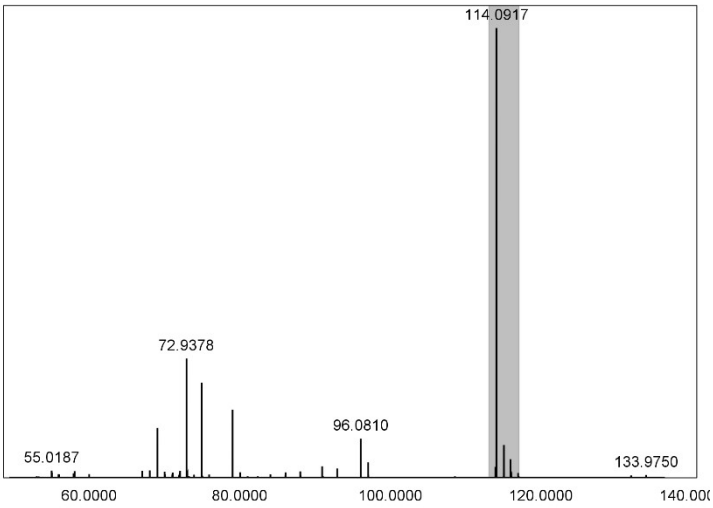

m/z =417

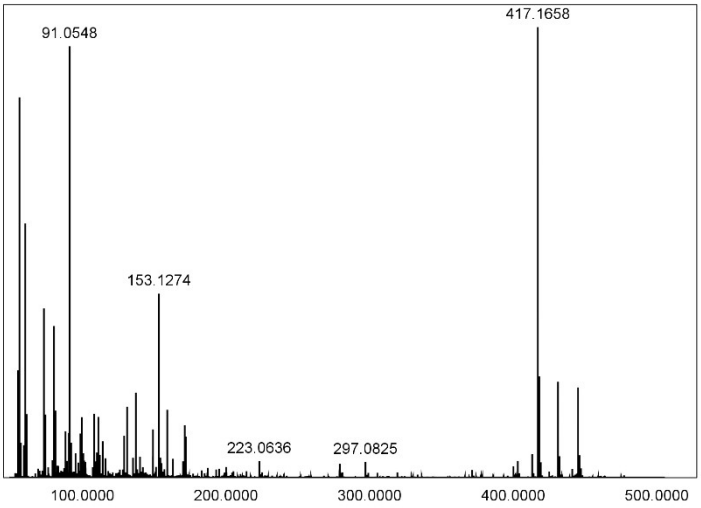

m/z =362

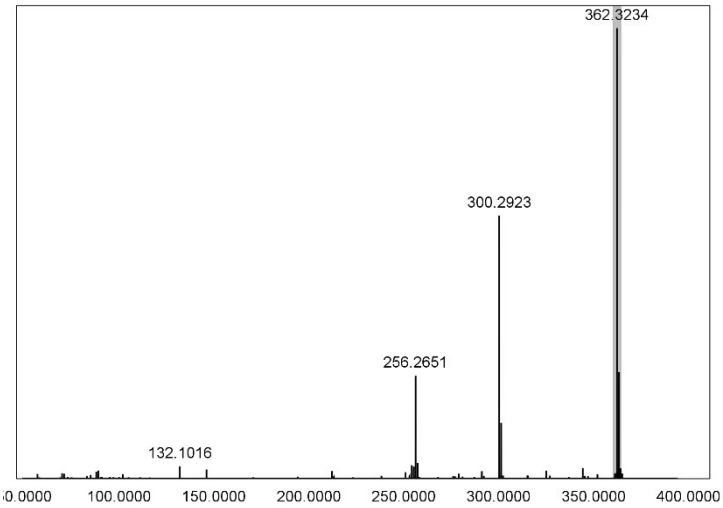

m/z =274

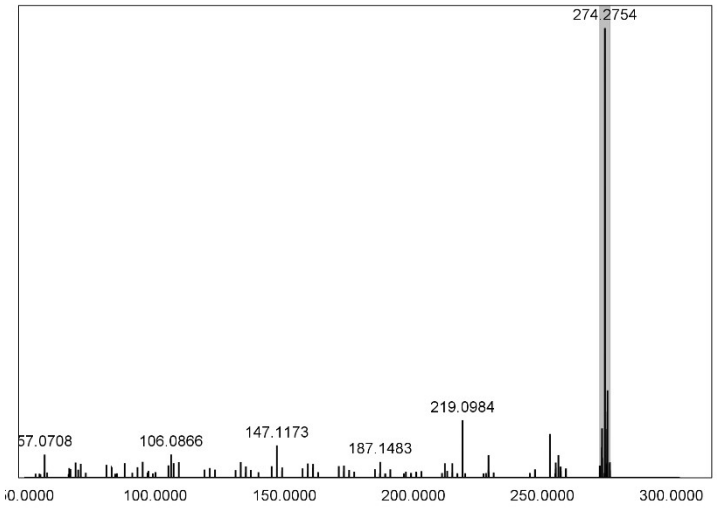

m/z =149

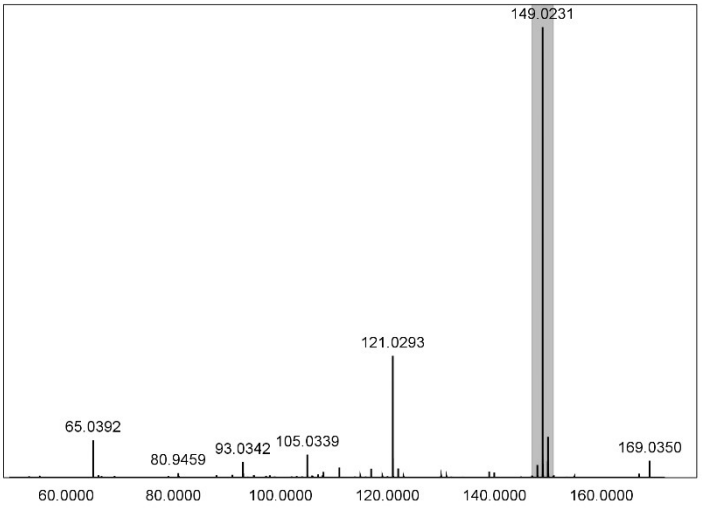

m/z =443

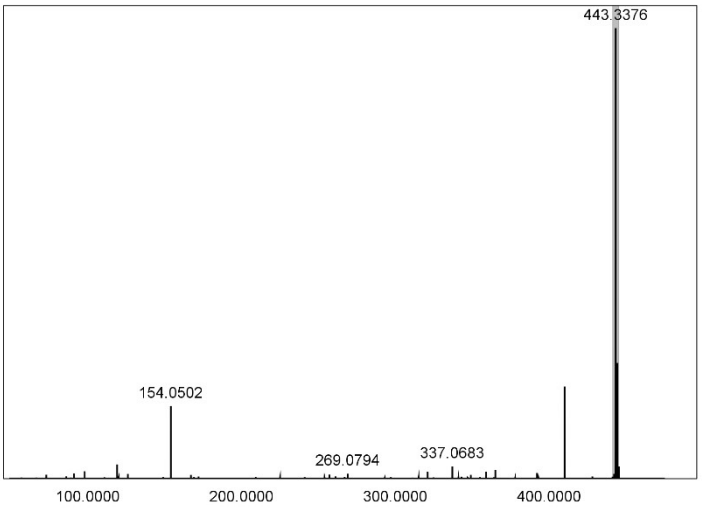

m/z =301

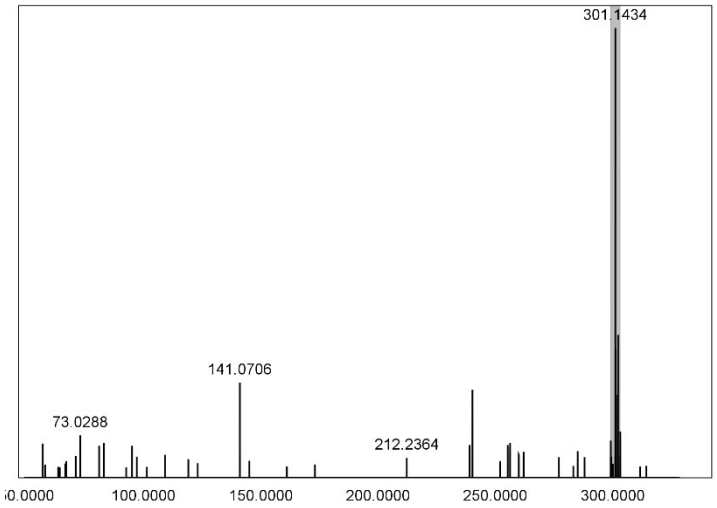

m/z =279

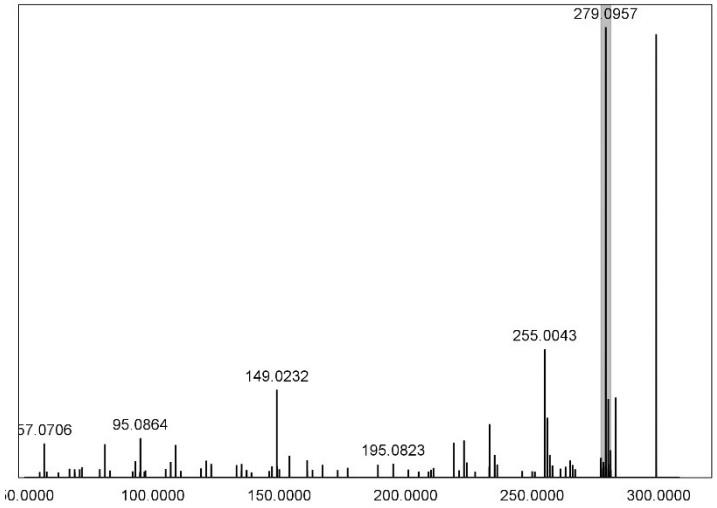

m/z =207

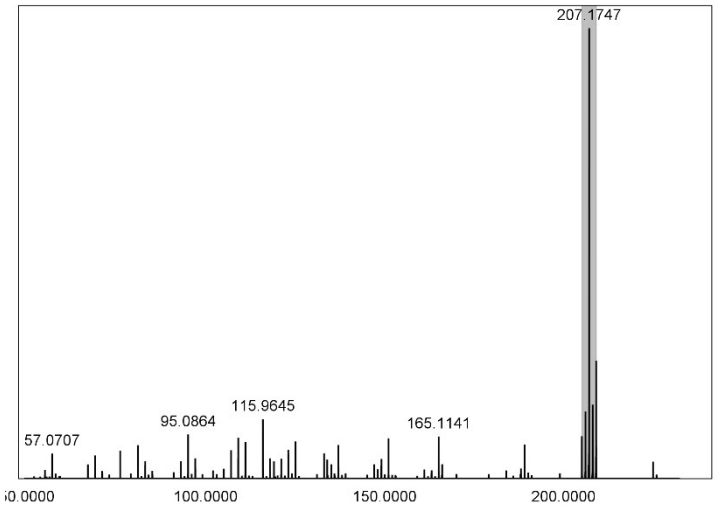

Supplementary references

1 W. Yang and R. G. Parr, *Proceedings of the National Academy of Sciences*, 1985, **82**, 6723–6726.
2 J.I. Martínez-Araya, Springer Nature Link, 2024, **62**, 461–475
3 T. Lu, F. Chen, Journal of Computational Chemistry, 2012, **33**: 580-592.